NTRK and *RET* fusion–directed therapy in pediatric thyroid cancer yields a tumor response and radioiodine uptake

Young Ah Lee,[1] Hyunjung Lee,[2,3] Sun-Wha Im,[3,4] Young Shin Song,[5] Do-Youn Oh,[6,7,8] Hyoung Jin Kang,[1,7,8] Jae-Kyung Won,[9] Kyeong Cheon Jung,[9] Dohee Kwon,[9] Eun-Jae Chung,[10] J. Hun Hah,[10] Jin Chul Paeng,[11] Ji-hoon Kim,[12] Jaeyong Choi,[2,3] Ok-Hee Kim,[13] Ji Min Oh,[14] Byeong-Cheol Ahn,[14] Lori J. Wirth,[15] Choong Ho Shin,[1] Jong-Il Kim,[2,3,4,7] and Young Joo Park[3,5,16]

[1]Department of Pediatrics, Seoul National University Children's Hospital, Seoul National University College of Medicine, Seoul, Republic of Korea. [2]Department of Biomedical Sciences, Seoul National University Graduate School, Seoul, Republic of Korea. [3]Genomic Medicine Institute, Medical Research Center, Seoul National University, Seoul, Republic of Korea. [4]Department of Biochemistry and Molecular Biology, and [5]Department of Internal Medicine, Seoul National University College of Medicine, Seoul, Republic of Korea. [6]Medical Oncology, Department of Internal Medicine, Seoul National University Hospital (SNUH), Seoul, Republic of Korea. [7]Seoul National University Cancer Research Institute, Seoul, Republic of Korea. [8]Integrated Major in Innovative Medical Science, Seoul National University Graduate School, Seoul, Republic of Korea. [9]Department of Pathology, [10]Department of Otorhinolaryngology – Head and Neck Surgery, [11]Department of Nuclear Medicine, and [12]Department of Radiology, SNUH, Seoul National University College of Medicine, Seoul, Republic of Korea. [13]Lee Gil Ya Cancer and Diabetes Institute, Gachon University College of Medicine, Incheon, Republic of Korea. [14]Department of Nuclear Medicine, School of Medicine, Kyungpook National University, Daegu, Republic of Korea. [15]Department of Medicine, Massachusetts General Hospital, Boston, Massachusetts, USA. [16]Department of Molecular Medicine and Biopharmaceutical Sciences, Graduate School of Convergence Science and Technology, Seoul National University, Seoul, Republic of Korea.

BACKGROUND. Molecular characterization in pediatric papillary thyroid cancer (PTC), distinct from adult PTC, is important for developing molecularly targeted therapies for progressive radioiodine-refractory (^{131}I-refractory) PTC.

METHODS. PTC samples from 106 pediatric patients (age range: 4.3–19.8 years; *n* = 84 girls, *n* = 22 boys) who were admitted to SNUH (January 1983–March 2020) were available for genomic profiling. Previous transcriptomic data from 125 adult PTC samples were used for comparison.

RESULTS. We identified genetic drivers in 80 tumors: 31 with fusion oncogenes (*RET* in 21 patients, *ALK* in 6 patients, and *NTRK1/3* in 4 patients); 47 with point mutations ($BRAF^{V600E}$ in 41 patients, $TERT^{C228T}$ in 2 patients [1 of whom had a coexisting $BRAF^{V600E}$], and *DICER1* variants in 5 patients); and 2 with amplifications. Fusion oncogene PTCs, which are predominantly detected in younger patients, were at a more advanced stage and showed more recurrent or persistent disease compared with $BRAF^{V600E}$ PTCs, which are detected mostly in adolescents. Pediatric fusion PTCs (in patients <10 years of age) had lower expression of thyroid differentiation genes, including *SLC5A5*, than did adult fusion PTCs. Two girls with progressive ^{131}I-refractory lung metastases harboring a *TPR-NTRK1* or *CCDC6-RET* fusion oncogene received fusion-targeted therapy; larotrectinib and selpercatinib decreased the size of the tumor and restored ^{125}I radioiodine uptake. The girl with the *CCDC6-RET* fusion oncogene received ^{131}I therapy combined with selpercatinib, resulting in a tumor response. In vitro ^{125}I uptake and ^{131}I clonogenic assays showed that larotrectinib inhibited tumor growth and restored radioiodine avidity.

CONCLUSIONS. In pediatric patients with fusion oncogene PTC who have ^{131}I-refractory advanced disease, selective fusion-directed therapy may restore radioiodine avidity and lead to a dramatic tumor response, underscoring the importance of molecular testing in pediatric patients with PTC.

FUNDING. The Ministry of Science, ICT and Future Planning (NRF-2016R1A2B4012417 and 2019R1A2C2084332); the Korean Ministry of Health and Welfare (H14C1277); the Ministry of Education (2020R1A6A1A03047972); and the SNUH Research Fund (04-2015-0830).

TRIAL REGISTRATION. Two patients received fusion-targeted therapy with larotrectinib (NCT02576431; NAVIGATE) or selpercatinib (LOXO-RET-18018).

▶ Related Commentary: https://doi.org/10.1172/JCI152696

Authorship note: YAL and HL contributed equally to this work. YJP and JIK co-supervised this work.
Conflict of interest: The authors have declared that no conflict of interest exists.

Submitted: October 5, 2020; **Accepted:** July 6, 2021; **Published:** September 15, 2021.
Reference information: *J Clin Invest*. 2021;131(18):e144847. https://doi.org/10.1172/JCI144847.

Table 1. Comparison of clinicopathological characteristics between pediatric patients with PTC harboring the fusion oncogene and those with *BRAF*^{V600E} PTC

	Total patients (*n* = 106)	Fusion PTCs (*n* = 31)	*BRAF*^{V600E} PTCs (*n* = 41)	*P* value (fusion vs. *BRAF*^{V600E})
Age (yr)	14.3 ± 3.8	11.1 ± 4.2	16.3 ± 2.3	<0.001
Age group (<10/10–14/15–19 yr), *n* (%)	14/40/52 (13.2/37.7/49.1)	13/11/7 (41.9/35.5/22.6)	0/11/30 (0/26.8/73.2)	<0.001
Sex (M/F), *n* (%)	22/84 (20.8/79.2)	6/25 (19.4/ 80.6)	6/35 (14.6/85.4)	0.751
Previous history of radiotherapy (yes/no), *n* (%)	9/97 (8.5/91.5)	3/28 (9.7/90.3)	1/40 (2.4/97.6)	0.308
Thyroidectomy (total thyroidectomy/lobectomy)	97/9 (91.5/8.5)	30/1 (96.8/3.2)	38/3 (92.7/7.3)	0.629
LN dissection, total (yes/no), *n* (%)	83/22 (79.3/20.9)[A]	28/3 (90.3/9.7)	33/7 (82.5/17.5)[A]	0.496
Lateral LN dissection (yes/no), *n* (%)	46/56 (45.1/54.9)[A]	22/9 (71.0/29.0)	11/26 (29.7/70.3)[A]	0.001
Radioiodine therapy (yes/no), *n* (%)	71/31 (69.6/30.4)[A]	27/4 (87.1/12.9)	23/17 (57.5/42.5)[A]	0.009
PTC subtype (classic variant/diffuse sclerosing variant/other subtypes[C]), *n* (%)	75[B]/14/15[C] (72.1/13.5/14.4)[A]	16/13/2 (51.6/41.9/6.5)	35/0/4 (89.7/0/10.3)[A]	0.025
Size (cm)	2.1 ± 1.3[A]	2.8 ± 1.5	1.4 ± 1.0[A]	<0.001
Size (>2 cm/ ≤2 cm), *n* (%)	46/56 (45.1/54.9)[A]	20/11 (64.5/35.5)	10/28 (26.3/73.7)[A]	0.002
Multifocality (yes/no), *n* (%)	40/65 (38.1/61.9)[A]	14/17 (45.2/43.8)	13/27 (32.5/67.5)[A]	0.329
ETE (yes/no), *n* (%)	70/30 (70.0/30.0)[A]	26/5 (83.9/16.1)	23/15 (60.5/39.5)[A]	0.028
No/minimal/gross, *n* (%)	30/45/24 (30.0/45.0/25.0)[A]	4/17/9 (13.3/56.7/30.0)	15/17/6 (39.5/44.7/15.8)[A]	0.020
LN metastasis (yes/no), *n* (%)	74/27 (73.3/26.7)[A]	29/2 (93.5/6.5)	26/12 (68.4/31.6)[A]	0.015
Lateral LN metastasis (yes/no), *n* (%)	24/73 (24.7/75.3)[A]	11/20 (35.5/64.5)	6/29 (17.1/82.9)[A]	0.101
Lung metastasis (yes/no), *n* (%)	20/83 (19.4/80.6)[A]	13/18 (41.9/58.1)	1/39 (2.5/97.5)[A]	<0.001
Follow-up yr, median (range)	7.3 (0.3–37.3)	4.8 (0.9–34.3)	8.0 (0.6–37.3)	0.106
Disease outcome at any event (NED/BCD/SD[D], *n* (%)	53/10/34 (54.6/10.3/35.1)[A]	6/6/17(20.7/20.7/58.6)[A]	27/4/6 (73.0/10.8/16.2)[A]	<0.001
Disease outcome at last follow-up (NED/BCD/SD[D], *n* (%)	60/15/22 (61.9/15.5/22.7)[A]	8/6/15 (27.6/20.7/51.7)[A]	29/7/1 (78.4/18.9/2.7)[A]	<0.001

Data are expressed as the mean ± standard deviation or as a percentage. [A]Number is less than the total number indicated in the column heading. [B]Two of the 75 patients had multifocal PTCs harboring different subtypes (classic variant and follicular variant, and classic variant and solid variant, respectively). [C]Other subtypes include 9 follicular variant, 2 solid variant, 1 tall cell variant, and 1 hobnail variant. [D]Disease outcomes were categorized as NED, BCD, and persistent or recurrent SD. NED, absence of structural abnormalities on imaging and undetectable serum thyroglobulin levels (suppressed or stimulated) for 12 months or longer until the last follow-up; SD, presence of structural abnormalities; BCD, detectable suppressed or stimulated thyroglobulin levels in the absence of structural abnormalities on imaging modalities. Stable and progressive disease were defined according to RECIST. F, females; M, males.

Introduction

Pediatric papillary thyroid cancers (PTCs) have distinct genetic alterations and a higher proportion of gene fusions compared with adult PTCs, in which point mutations predominate (1).

Previous methods to detect *BRAF*^{V600E}, *RAS*, or *RET/PTC* gene alterations identified driver alterations in less than half of pediatric PTCs (2). However, next-generation sequencing (NGS) has increased the detection rate of genetic drivers in sporadic cases by more than 60% (3–7). A significant proportion of fusion oncogenes have been detected (20%–60%), as with radiation-associated thyroid cancers (8). This high frequency of oncogenic fusion may be important in the pathogenesis of pediatric PTCs and could facilitate the selection of patients for recently developed, highly selective and potent fusion-targeted agents (9, 10). Moreover, identification of transcriptomic characteristics may help determine the pathogenesis and biological behavior of pediatric PTCs and differentiate them from adult PTCs. Previous molecular studies of pediatric PTCs have generally been too small to generate age-associated genomic profiles, and transcriptomic information on these tumors is limited.

In this study, we comprehensively characterized age-associated genetic alterations in a large series of pediatric PTCs. Furthermore, we performed transcriptome analyses of pediatric PTCs and compared these profiles with those reported for adult PTCs (11). On the basis of these data, we investigated the role of the *NTRK* and *RET* fusion–targeted agents, larotrectinib and selpercatinib, respectively, in the inhibition of tumor growth and restoration of radioiodine uptake in progressive radioiodine-refractory (^{131}I-refractory) PTCs in young children.

Results

Age-associated genetic alterations in pediatric PTCs. The clinicopathological characteristics and genetic analyses of 106 Korean patients (age range: 4.3–19.8 years; *n* = 84 girls and *n* = 22 boys) are summarized in Table 1 and Figure 1. We identified genomic alterations in 80 of these patients, including 31 with oncogenic fusions (*NTRK1/3* in 4 patients, *RET* in 21 patients, and *ALK* in 6 patients), 47 with point mutations (*BRAF*^{V600E} in 41 patients, *TERT*^{C228T} in 2 patients [1 of whom had a coexisting *BRAF*^{V600E}], and *DICER1* variants in 5 patients), and 2 with *FGFR1* or *EGFR* amplifications (Supplemental Tables 1 and 2; supplemental material available online with this article; https://doi.org/10.1172/JCI144847DS1). Detailed information on the fusion partner genes, breakpoints, and methods to detect each fusion oncogene are described in Table 2,

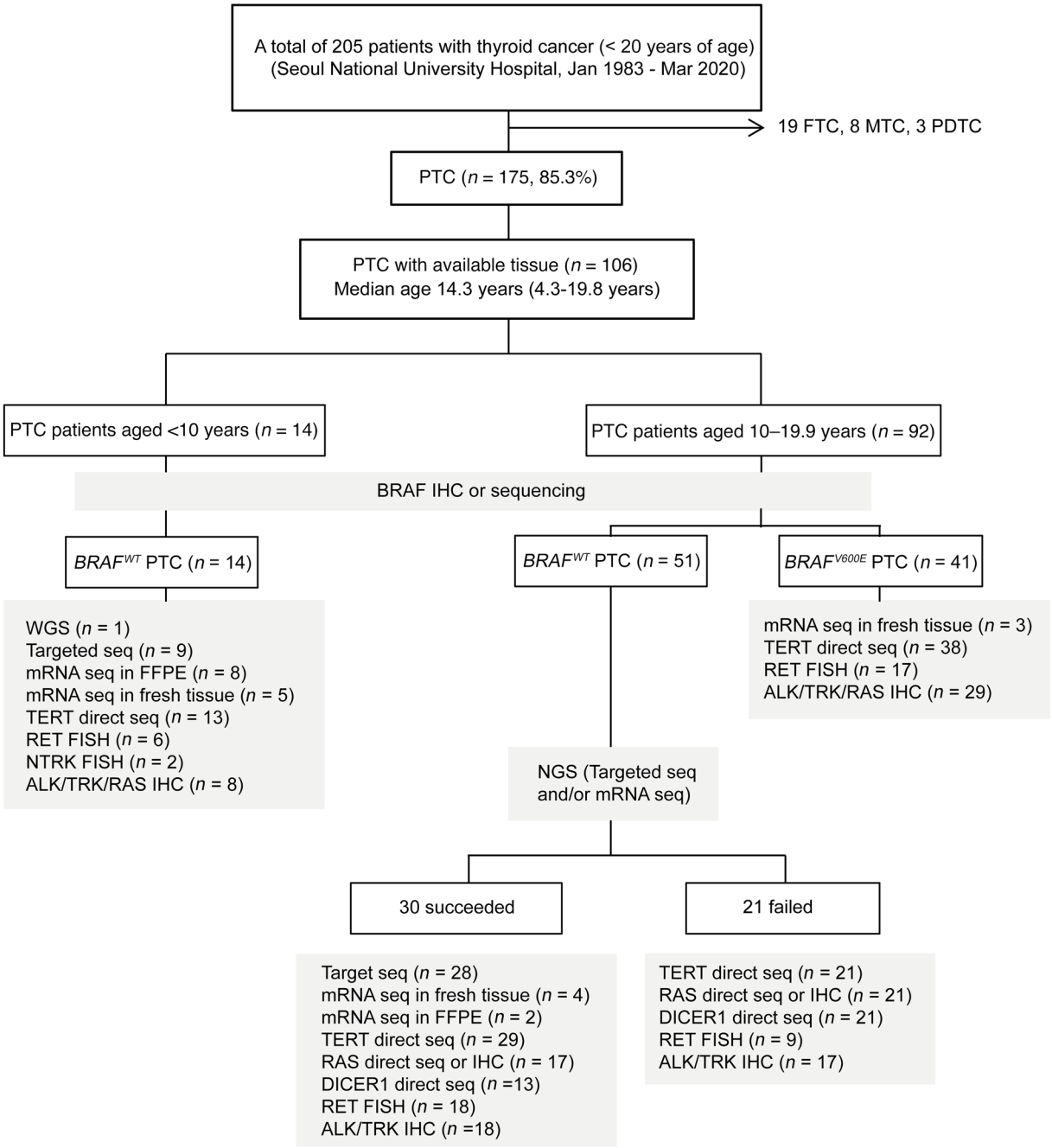

Figure 1. Flow diagram describing comprehensive genomic profiling of pediatric PTC samples. Tumor tissue samples (n = 106) from pediatric patients with PTC (n = 84 girls, n = 22 boys; median age: 14.3 years; range: 4.3–19.8 years) were analyzed to profile genetic alterations using WGS, targeted sequencing, mRNA sequencing, direct sequencing, FISH, and/or IHC depending on the availability of each tissue. FTC, follicular thyroid cancer; MTC, medullary thyroid cancer; PDTC, poorly differentiated thyroid cancer.

Supplemental Table 3, and Supplemental Figure 1. *H/K/NRAS* mutations were not identified in any of the tested tumors. Among 9 patients who underwent radiotherapy, we identified a genetic driver in 7 of them (2 *RET*, 1 *ALK*, 1 $BRAF^{V600E}$, 1 $DICER1^{D1709G}$ with coexisting loss of heterozygosity at multiple chromosomal loci and 2 amplifications; Supplemental Table 1).

In the 3 groups — patients under 10 years of age (n = 14), patients 10–14 years old (n = 40), and patients 15–19 years old (n = 52) — the proportions of fusion oncogenes were 92.9%, 27.5%, and 13.5%, respectively, whereas the point mutation rates were 7.1%, 30.0%, and 65.4% (Figure 2A), with $BRAF^{V600E}$ rates of 0%, 27.3%, and 57.7%, respectively. The frequency of each gene according to age is shown in Figure 2B and Supplemental Table 2. In particular, among 14 young children below 10 years of age, 13 harbored a fusion oncogene (9 *RET*, 2 *NTRK*, and 2 *ALK*) and 1 had a $TERT^{C228T}$ mutation. The pooled analysis (Supplemental Table 4)

Table 2. Clinicopathological presentation and disease outcomes in pediatric patients with PTC harboring a fusion oncogene

ID	Age (yr)	Sex	Sporadic PTC or radiotherapy[A]	PTC subtype	Genetic alteration	Size (cm)	Multifocality	ETE	LN metastasis	Distant metastasis	Follow-up (yr)	Disease outcome[C] (any event)	Disease outcome[C] (at last follow-up)
1	4.3	F	Sporadic	cPTC	TPR-NTRK1	3.6	No	Minimal	Yes	Lung	5.3	SD (persist, LN and lung)	SD (progress, LN and lung)
2	5.2	F	Sporadic	FVPTC, infiltrative	ETV6-NTRK3	2.1	No	Minimal	Yes	No	5.0	BCD	BCD
3	10.4	F	Sporadic	FVPTC, infiltrative	ETV6-NTRK3	1.5	No	N/A	Yes	Yes	2.2	SD (persist, LN and lung)	SD (persist, lung)
4	14.2	F	Sporadic	cPTC	TPM3-NTRK1	2.1	No	No	Yes	No	0.6	Ongoing	Ongoing
5	5.1	F	Sporadic	cPTC	VCL-RET	2.5	No	Gross	Yes	Lung	8.2	NED	NED
6	6.4	M	Sporadic	DSV-PTC	NCOA4-RET	1.3	Yes	Minimal	Yes	No	7.2	SD (recur)	NED
7	7.1	F	Sporadic	DSV-PTC	TRIM24-RET	1.5	No	No	Yes	Lung	8.8	SD (persist, lung)	SD (persist, lung)
8	7.4	F	Sporadic	DSV-PTC	CCDC6-RET	2.8	No	Minimal	Yes	Lung	3.5	SD (persist, LN and lung)	SD (progress, LN and lung)
9	7.6	F	Sporadic	cPTC	RET-NCOA4	1.0	No	Gross	Yes	No	34.3	SD (recur)	NED
10	7.8	M	Radiotherapy[A]	cPTC	NCOA4-RET	2.6	Yes	Gross	Yes	No	7.0	BCD	BCD
11	9.0	M	Sporadic	DSV-PTC	ERC1-RET	7.0	Yes	Minimal	Yes	Lung	3.4	SD (persist, lung)	SD (progress, lung)
12	9.6	M	Sporadic	cPTC	TRIM24-RET	2.4	No	Minimal	Yes	No	4.6	SD (recur)	BCD
13	9.9	M	Sporadic	DSV-PTC	NCOA4-RET	1.6	No	Minimal	Yes	No	7.2	BCD	BCD
14	10.1	F	Sporadic	cPTC	NCOA4-RET	2.2	Yes	Gross	Yes	Lung	9.0	SD (persist, lung)	SD (persist, lung)
15	10.3	F	Sporadic	DSV-PTC	CCDC6-RET	2.5	Yes	Gross	Yes	Lung	9.5	SD (persist, LN and lung)	SD (persist, lung)
16	10.4	F	Sporadic	DSV-PTC	NCOA4-RET	4.1	Yes	Gross	Yes	No	2.5	SD (recur)	SD (recur)
17	10.5	F	Sporadic	DSV-PTC	CCDC6-RET	7·0	No	Minimal	Yes	No	1.7	SD (recur)	SD (recur)
18	13.3	F	Radiotherapy[A]	cPTC	CCDC6-RET	1.7	No	Minimal	No	No	4.8	NED	NED
19	13.7	F	Sporadic	DSV-PTC	ANK3-RET	3.5	No	Minimal	Yes	No	2.0	NED	NED
20	14.3	F	Sporadic	DSV-PTC	KTN1-RET	5.0	No	Gross	Yes	Lung	2.7	SD (persist, lung)	SD (persist, lung)
21	14.5	F	Sporadic	cPTC	CCDC6-RET	4.2	No	No	Yes	No	11.7	NED	NED
22	16.1	M	Sporadic	cPTC	CCDC6-RET	1.9	Yes	Minimal	Yes	No	10.7	BCD	BCD
23	16.1	F	Sporadic	DSV-PTC	CCDC6-RET	2.3	Yes	Minimal	Yes	Lung	3.1	SD (persist, lung)	SD (persist, lung)
24	17.2	F	Sporadic	cPTC	CCDC6-RET	0.9	No	No	No	No	13.2	NED	NED
25	18.9	F	Sporadic	DSV-PTC	CCDC6-RET	1.9	Yes	Minimal	Yes	No	3.2	BCD	BCD
26	4.5	F	Sporadic	DSV-PTC	STRN-ALK	3.3	Yes	Minimal	Yes	Lung	1.6	Ongoing	Ongoing
27	8.9	F	Sporadic	cPTC	EML4-ALK	1.4	Yes	Minimal	Yes	No	3.4	NED	NED
28	12.1	F	Sporadic	cPTC	*ALK*[B]	1.8	No	Minimal	Yes	Lung	8.8	SD (persist, lung)	SD (persist, lung)
29	15.6	F	Sporadic	cPTC	RBMS3-ALK	4.0	Yes	Gross	Yes	Lung	15.3	SD (persist, lung)	SD (persist, lung)
30	15.9	F	Sporadic	cPTC	*ALK*[B]	4.0	Yes	Gross	Yes	No	2.0	BCD	BCD
31	18.1	F	Sporadic	cPTC	*ALK*[B]	2.2	Yes	Gross	Yes	No	4.1	SD (persist, LN)	BCD

[A]Childhood cancer survivors who had received radiotherapy. [B]Fusions where no 5′ partner was specified. [C]Disease outcomes were categorized as NED, BCD, and persistent or recurrent SD. NED, absence of structural abnormalities on imaging and undetectable serum thyroglobulin levels (TSH-suppressed or -stimulated) for 12 months or longer until the last follow-up; SD, presence of structural abnormalities showing locally advanced and/or metastatic disease; BCD, detectable serum thyroglobulin levels (TSH-suppressed or -stimulated) in the absence of structural abnormalities on imaging modalities. Stable disease and progressive disease were defined according to RECIST. cPTC, classic variant PTC; FVPTC, follicular variant PTC; DSV-PTC, diffuse sclerosing variant PTC; persist, persistent; progress, progressive; recur, recurrent.

revealed similar trends among the patients under 10 years of age and patients 10–22 years of age (Figure 2, C and D).

Clinicopathological characteristics and outcomes according to the genetic alterations in pediatric PTCs. We found that oncogenic fusion PTCs were associated with a higher proportion of large tumors (>2 cm), extrathyroidal extension (ETE), and lymph node (LN) and lung metastasis compared with *BRAF*^{V600E} PTCs (Tables 1 and 2 and Supplemental Table 5). *RET* fusion PTC was predominantly a diffuse sclerosing variant (DSV) (55.0%), whereas *BRAF*^{V600E} PTC was mostly a classic variant (89.7%). The oncogenic fusion PTCs were categorized into 2 age groups: fusion PTCs in patients under 10 years of age (n = 13) and fusion PTCs in patients 10–19 years of age (n = 18), and *BRAF*^{V600E} PTCs were all in the 10–19 years age group (n = 41). The proportion of large tumors, ETE, LN or lung metastasis (Figure 2E), and biochemical disease (BCD) or structural disease (SD) (Figure 2F) significantly decreased from the group of patients under 10 years of age with fusion PTC, to the 10–19 years age groups with fusion PTC, and to the 10–19 years age groups with *BRAF*^{V600E} PTC. Among the 13 patients with persistent lung metastasis despite ^{131}I treatment (2 patients with *NTRK1*, 7 patients with *RET*, 2 patients with *ALK*, 1 patient with *DICER1*, and 1 patient with no driver identified), 10 patients maintained stable status, while 3 young children (P1 with a *TPR-NTRK1*, P8 with a *CCDC6-RET*, and P11 with an *ERC1-RET* fusion) had ^{131}I-refractory progressive disease (Table 2). P1 and P8 were exposed to the fusion-targeted kinase inhibitor described below. The other child, a 9-year-old boy (P11) with an *ERC1-RET* fusion, showed mixed responses resulting in a progressive decrease in radioiodine uptake uptake during repeated high-dose ^{131}I therapy (cumulative dose = 520 mCi, 5 times) (Supplemental Figure 2). He is currently planning to participate in a phase III clinical trial of fusion-targeted therapy.

Comparison of clinicopathological characteristics and outcomes between pediatric and adult PTCs. We compared the clinicopathological presentation and outcomes between pediatric and adult patients at Seoul National University Hospital (11) according to whether the genetic driver was a fusion oncogene (*NTRK1/3*, *RET*, or *ALK*) or *BRAF*^{V600E}. The pediatric fusion oncogen group (n = 31) had higher rates of ETE (Figure 2G) and BCD or SD (Figure 2H) than did the adult fusion oncogene group (n = 12). Although the adult *BRAF*^{V600E} group (n = 68) had a higher rate of LN metastasis than the pediatric *BRAF*^{V600E} group (n = 41), disease outcomes did not differ between the pediatric and adult *BRAF*^{V600E} groups (Supplemental Table 6 and Figure 2, G and H). Recurrence-free survival was significantly higher in the pediatric *BRAF*^{V600E} and adult *BRAF*^{V600E} groups compared with the pediatric fusion group (P <0.05 for both, Figure 2I) When our pediatric data were compared with those in The Cancer Genome Atlas (TCGA) database, including the adult fusion group (n = 42) and *BRAF*^{V600E} group (n = 241), we obtained similar results (Supplemental Table 7).

Comparison of gene expression levels between pediatric and adult PTCs. A more advanced presentation and worse outcome of oncogenic fusion PTCs and their predominance among younger patients imply distinct molecular characteristics that differ between pediatric and adult PTCs (12). The gene expression profiles of 9 oncogenic fusion PTCs from children clustered closer to those of the adult *BRAF*-like group, whereas adult PTCs harboring fusion oncogenes were scattered (Figure 3A) (11). Figure 3B shows age-associated clustering of oncogenic fusion PTCs. As indicated in Figure 3C and Supplemental Figure 3, pediatric oncogenic fusion PTC patients, particularly those in the group under 10 years of age, showed higher expression of MAPK signaling pathway genes (ERK score) and lower expression of genes related to thyroid differentiation (thyroid differentiation score [TDS]) than did the adult fusion PTC groups (11, 13). We also found higher ERK scores and lower TDSs in the pediatric *BRAF*^{V600E} group than in the adult *BRAF*^{V600E} group (Figure 3C). Transcriptomic expression analysis of individual TDS genes demonstrated that several genes, including *SLC5A5*, *SLC26A4*, *SLC5A8*, *DIO1*, and *DIO2*, tended to have lower expression levels in pediatric fusion PTCs (<10 years of age) compared with adult fusion PTCs (Figure 3D). Notably, the expression of *SLC5A5* (sodium-iodide symporter [NIS]), which is an important determinant of ^{131}I avidity, also decreased in childhood fusion PTCs. However, the difference was not significant, given the limited number of fresh tissues; therefore, we also explored the lower TDSs and lower expression levels of the *SLC5A5* gene in pediatric fusion tumors compared with normal tissues by analyzing the formalin-fixed, paraffin-embedded (FFPE) samples of 8 fusion PTCs from young children (Figure 3E). Remarkably, the two ^{131}I-refractory progressive PTC patients had very low expression of *SLC5A5* in their tumor tissues (P1 in Figure 3D, and P8 in Figure 3E).

Larotrectinib decreases the tumor size and restores radioiodine uptake in ^{131}I-refractory progressive metastatic TPR-NTRK1 fusion–positive pediatric PTCs. A 4.3-year-old girl (P1 in Table 2) was diagnosed with a 3.6 cm classic variant PTC with extensive LN involvement and lung metastases. She underwent a total thyroidectomy and neck dissection, followed by administration of 30 mCi (0.06 GBq/kg) ^{131}I. The post-treatment whole-body scan (WBS) revealed remnant thyroid uptake only (Figure 4A, upper left). No ^{131}I uptake was identified on the post-treatment scan after the second dose of 30 mCi (Figure 4A, upper right), despite locoregional recurrence and progressive lung disease (Figure 4B, baseline). The patient's thyrotropin-stimulating hormone (TSH-stimulated) serum thyroglobulin level was 1150 ng/mL. We identified a *TPR-NTRK1* rearrangement and initiated larotrectinib at 100 mg orally, twice daily (per the NAVIGATE trial protocol; NCT02576431). CT revealed a dramatic improvement in the LN and lung metastases after 4 weeks (Figure 4B) and a complete response at 21 months, according to Response Evaluation Criteria in Solid Tumors (RECIST), version 1.1. After 12 weeks of therapy, radioiodine uptake was shown to be restored in the neck and lungs by a diagnostic ^{123}I scan (Figure 4A, lower left and right). The patient did not undergo ^{131}I therapy because of her participation in the clinical trial and has remained responsive, without dose-limiting toxicity at 41 months (Figure 4B).

Selpercatinib decreases the tumor size and restores radioiodine uptake in ^{131}I-refractory progressive metastatic CCDC6-RET fusion–positive pediatric PTC. A 7.4-year-old girl (P8 in Table 2) was diagnosed with a 2.8 cm DSV PTC with LN involvement and lung metastases. She underwent total thyroidectomy and neck dissection, followed by the administration of 50 mCi (0.11 GBq/kg) ^{131}I. The post-treatment WBS identified minimal lung uptake (Figure 4C, left). Her TSH-stimulated serum thyroglobulin level

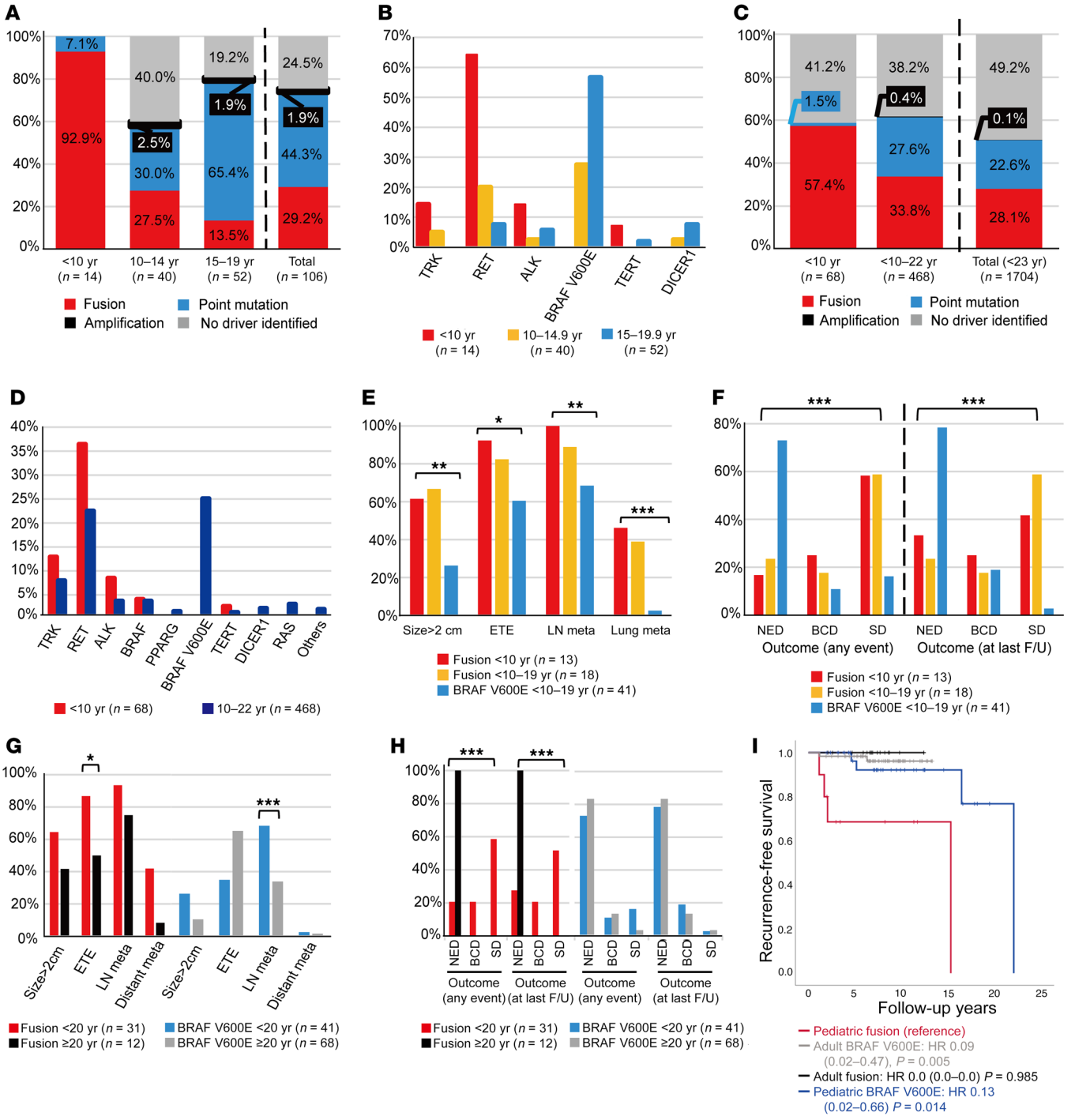

Figure 2. Age-associated genetic profiles of pediatric PTCs and comparison of the clinicopathological presentation and disease outcomes between fusion oncogene and *BRAF*^{V600E} PTCs. (**A**–**D**) Age-associated proportions of fusion oncogenes, point mutations, and genetic drivers among the pediatric patients in this study (**A** and **B**; patients aged <10 years, *n* = 14; 10–14 years; *n* = 40, and 15–19 years, *n* = 52) and a pooled analysis of 1704 patients under 23 years of age (**C** and **D**; patients aged <10 years, *n* = 68 and patients aged 10–22 years, *n* = 468, plus other patients without detailed age information). Comparison of the clinicopathological presentation (**E**) and disease outcomes (**F**) among the 3 pediatric groups: fusion PTCs in patients <10 years of age (*n* = 13), fusion PTCs in patients 10–19 years of age (*n* = 18), and *BRAF*^{V600E} PTCs in all patients 10–19 years of age (*n* = 41). Comparison of the clinicopathological presentation (**G**) and disease outcomes (**H**) between the pediatric fusion (*n* = 31) and adult fusion (*n* = 12) groups, and between the pediatric *BRAF*^{V600E} (*n* = 41) and adult *BRAF*^{V600E} (*n* = 68) groups. Categorical variables were compared between the 2 groups using the χ^2 or Fisher's exact test, whereas the χ^2 test for trend or logistic regression was used for comparisons among the 3 groups (*$P < 0.05$, **$P < 0.01$, and ***$P < 0.001$). (**I**) Recurrence-free survival was compared among these 4 groups with reference to the pediatric fusion group. Recurrence-free survival plots were constructed using the Kaplan-Meier method, and groups were compared using the Cox proportional hazards model. The HRs, 95% CIs, and *P* values are reported in the figure. F/U, follow-up; meta, metastasis.

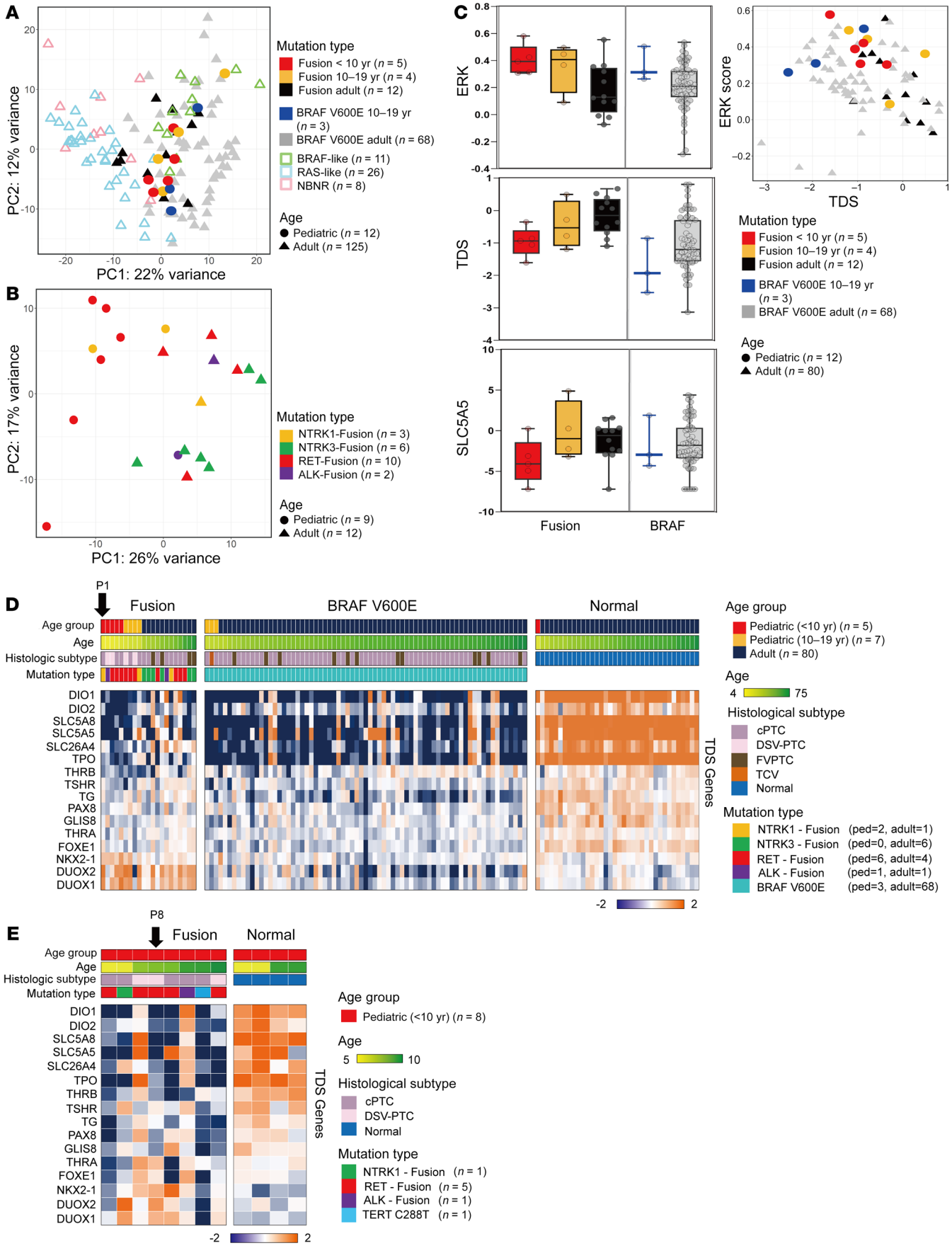
A
PC2: 12% variance
PC1: 22% variance
Mutation type
Fusion < 10 yr (n = 5)
Fusion 10–19 yr (n = 4)
Fusion adult (n = 12)
BRAF V600E 10–19 yr (n = 3)
BRAF V600E adult (n = 68)
BRAF-like (n = 11)
RAS-like (n = 26)
NBNR (n = 8)
Age
Pediatric (n = 12)
Adult (n = 125)
B
PC2: 17% variance
PC1: 26% variance
Mutation type
NTRK1-Fusion (n = 3)
NTRK3-Fusion (n = 6)
RET-Fusion (n = 10)
ALK-Fusion (n = 2)
Age
Pediatric (n = 9)
Adult (n = 12)
C
ERK
TDS
SLC5A5
Fusion
BRAF
ERK score
TDS
Mutation type
Fusion < 10 yr (n = 5)
Fusion 10–19 yr (n = 4)
Fusion adult (n = 12)
BRAF V600E 10–19 yr (n = 3)
BRAF V600E adult (n = 68)
Age
Pediatric (n = 12)
Adult (n = 80)
D
P1
Fusion
BRAF V600E
Normal
Age group
Age
Histologic subtype
Mutation type
DIO1
DIO2
SLC5A8
SLC5A5
SLC26A4
TPO
THRB
TSHR
TG
PAX8
GLIS8
THRA
FOXE1
NKX2-1
DUOX2
DUOX1
TDS Genes
Age group
Pediatric (<10 yr) (n = 5)
Pediatric (10–19 yr) (n = 7)
Adult (n = 80)
Age
4
75
Histological subtype
cPTC
DSV-PTC
FVPTC
TCV
Normal
Mutation type
NTRK1 - Fusion (ped=2, adult=1)
NTRK3 - Fusion (ped=0, adult=6)
RET - Fusion (ped=6, adult=4)
ALK - Fusion (ped=1, adult=1)
BRAF V600E (ped=3, adult=68)
E
P8
Fusion
Normal
Age group
Pediatric (<10 yr) (n = 8)
Age
5
10
Histological subtype
cPTC
DSV-PTC
Normal
Mutation type
NTRK1 - Fusion (n = 1)
RET - Fusion (n = 5)
ALK - Fusion (n = 1)
TERT C288T (n = 1)

Figure 3. Comparison of expression signatures between pediatric and adult PTCs. (**A** and **B**) Results of K-means clustering (obtained via principal component analysis). (**A**) Comparison between 12 pediatric PTCs (9 fusion oncogenes and 3 *BRAF*^{V600E} PTCs) and 125 adult PTCs, including BRAF-like, RAS-like, and non-BRAF–non-RAS (NBNR). (**B**) Comparison between pediatric (n = 9) and adult (n = 12) PTCs with fusion oncogenes. The patients' ages and mutation types are represented by shapes and colors, respectively. (**C**) Box plots (left) show the ERK score, TDS, and SLC5A5 (NIS) analysis results. Scatterplot (right) shows the results of the TDS and ERK score analysis. (**D**) Heatmap shows the expression levels of 16 TDS genes associated with thyroid function and metabolism. Comparison of TDS gene expression levels between the pediatric (ped) and adult fusion groups and between the pediatric and adult *BRAF*^{V600E} groups using fresh-frozen tissue samples. cPTC, classic variant PTC; DSV-PTC, diffuse sclerosing variant PTC; FVPTC, follicular variant PTC; TCV, tall cell variant PTC. (**E**) Comparison of TDS genes between pediatric PTCs and normal thyroid tissues based on an analysis of FFPE samples. Two young girls (P1 and P8) with progressive ^{131}I-refractory lung metastasis had low expression of *SCL5A5* in their tumor tissues.

was 5990 ng/mL. After 4 months, locoregional recurrence and progressive lung metastases were detected (Figure 4D, baseline). We identified a *CCDC6-RET* rearrangement and initiated selpercatinib at 80 mg orally, twice daily (LOXO-RET-18018). The lung lesions were markedly decreased in size according to a chest radiograph on day 10 (Figure 4D, upper right). Since achieving a partial response after 4 weeks according to RECIST, version 1.1 (Figure 4D, lower middle), the patient has remained responsive, with no dose-limiting toxicity. Radioiodine uptake was restored in the lung on a diagnostic ^{123}I scan at 5 months (Figure 4C, middle), which enabled administration of 60 mCi (0.11GBq/kg) ^{131}I combined with selpercatinib, leading to remarkable radioiodine uptake in the entire lung field at 13 months (Figure 4C, right) and a TSH-stimulated serum thyroglobulin level of 1930 ng/mL. ^{131}I therapy of 60 mCi (0.11 GBq/kg) was additionally administered after 19 months of the selpercatinib therapy, leading to persistent radioiodine uptake in the lung field with a TSH-stimulated serum thyroglobulin level of 855 ng/mL. CT revealed stable lung disease at 29 months (Figure 4D, lower right).

In vitro effects of larotrectinib on tumor growth and radioiodine uptake capacity. The restoration of radioiodine uptake in ^{131}I non-avid lesions after larotrectinib and selpercatinib treatment implies that these selective inhibitors not only abrogate cellular proliferation but also induce the restoration of iodine uptake and processing in these cancers, similar to what was previously reported on MAPK inhibitors (14–16).

In vitro experiments showed that basal ^{125}I uptake was markedly decreased in Nthy$^{TPR\text{-}NTRK}$ cells compared with control Nthy^{WT} cells, but was restored by larotrectinib treatment (Figure 5A and Supplemental Figure 4, A and B). This larotrectinib-induced restoration was mediated by the NIS, as indicated by the effects being blocked by potassium perchlorate ($KClO_4$), a competitive inhibitor of iodide transport through the NIS (Figure 5A and Supplemental Figure 4C). A trend toward increased expression of the NIS at the mRNA and protein levels was associated with larotrectinib treatment in Nthy$^{TPR\text{-}NTRK}$ cells (Figure 5, B and C, and Supplemental Figure 4D), but not in Nthy^{WT} cells (Supplemental Figure 4D). To evaluate whether larotrectinib treatment enhances the therapeutic effect of ^{131}I, we pretreated Nthy$^{TPR\text{-}NTRK}$ cells with larotrectinib followed by 100 μCi of ^{131}I. Although ^{131}I alone did not suppress the colony-forming ability in Nthy$^{TPR\text{-}NTRK}$ cells, larotrectinib alone inhibited colony formation. Moreover, the combination of ^{131}I and larotrectinib further enhanced the inhibition of colony forming (Figure 5D and Supplemental Figure 4E).

Discussion

Our comprehensive genomic analysis revealed age-associated driver profiles of pediatric PTC. Oncogenic fusions predominated in children with PTCs under 10 years of age, after which the frequency decreased to levels similar to those seen in adults. Furthermore, the incidence of driver point mutations increased with age and became common in adolescents aged 15–19 years, as in adults. Pediatric patients with oncogenic fusion PTCs presented with more advanced disease and had worse outcomes than did pediatric patients with *BRAF*^{V600E} PTCs. The transcriptomic data showed that pediatric oncogenic fusion PTCs in young children under 10 years of age had a lower TDS (including NIS expression) than did adult fusion PTCs. *NTRK* and *RET* fusion–targeted therapy with larotrectinib or selpercatinib yielded a remarkable tumor response and restored radioiodine uptake in 2 pediatric patients with ^{131}I-refractory progressive PTCs harboring *TPR-NTRK1* and *CCDC6-RET* fusion oncogenes, respectively.

The detection rate of genetic alterations was 75.5% in our pediatric PTC population with the use of NGS, FISH, and IHC. To our knowledge, this was the largest pediatric study to date showing age-associated genetic alterations, consistent with a pooled analysis of previously reported cases, including a large recent pediatric study of 93 patients that used DNA and RNA-Seq (Supplemental Table 4) (2, 17). Oncogenic fusions accounted for the majority of cases among children under 10 years of age, while *BRAF*^{V600E} was the most common driver in adolescents, with a frequency similar to that seen in adults (13, 18). *DICER1* was the second most common point mutation, a finding consistent with a recent pediatric study (19). However, *TERT* promoter and *RAS* mutations were uncommon, in line with previous pediatric reports (Supplemental Table 4) (2–7, 17, 20–22).

The etiology of age-associated genetic alterations remains unexplained, although chromosomal rearrangements have a strong association with exposure to ionizing radiation, whereas *BRAF*^{V600E} point mutations may be linked to excess dietary iodine intake or exposure to chemical elements in volcanic areas (23). DNA fragility and repair defects have been suggested as mechanisms for radiation-induced genetic changes or spontaneous oncogenic fusion (4, 5, 24). The thyroid cells of young children may be more susceptible to the effects of ionizing radiation and/or lose key factors in the DNA repair machinery, leading to uncoupled double-stranded breaks and translocation with partner genes (24). Analysis of post- analysis of post-Chernobyl thyroid cancers showed that the mean age at radiation exposure was lower in patients with tumors harboring oncogenic fusion genes (7.1 years) than in those with tumors harboring point mutations (10.9 years) (25). As almost all patients under 10 years of age with sporadic PTC also harbored oncogenic fusions in this study, further analysis to determine as-yet unknown risk factors for the development of fusions is needed.

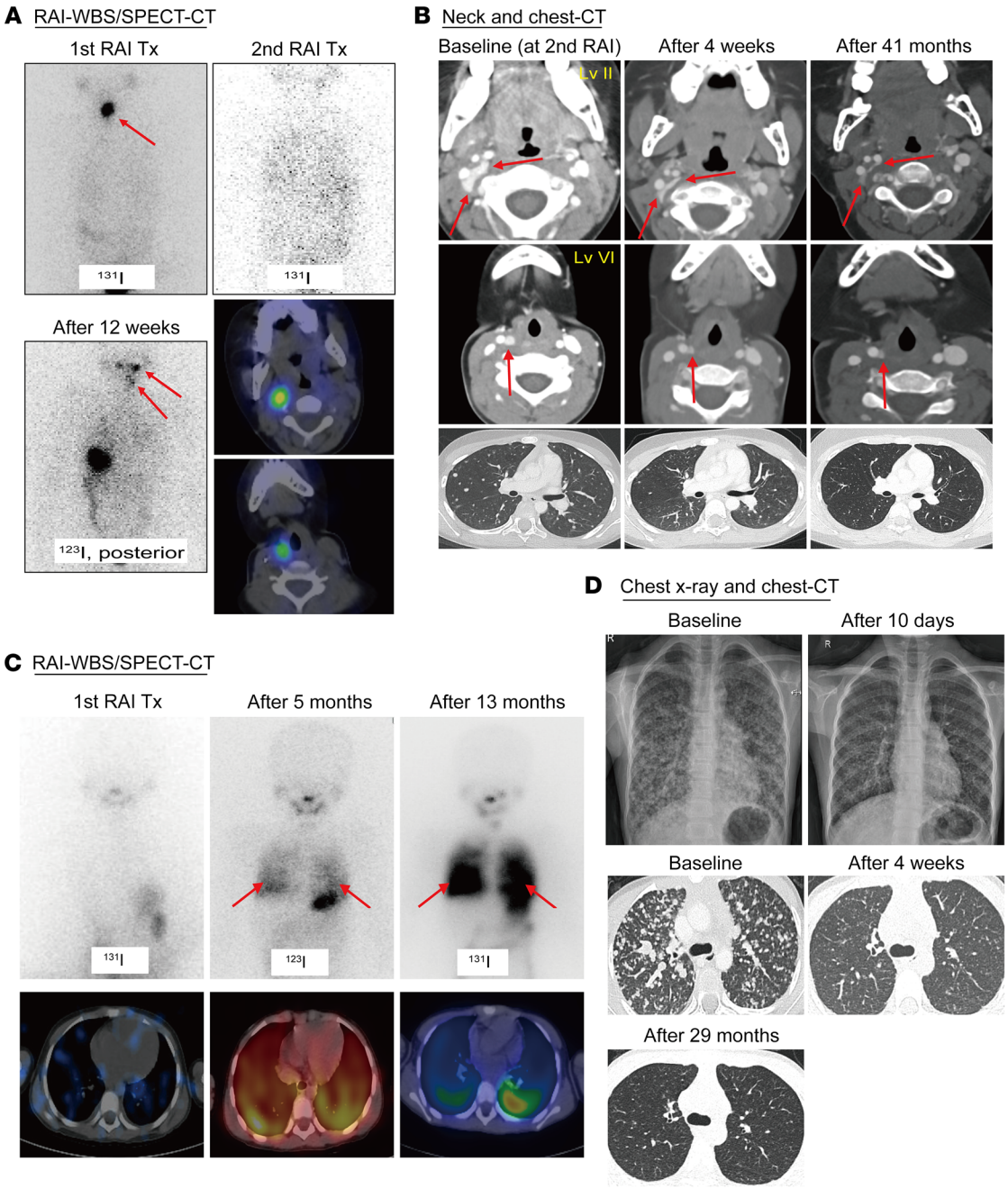

Figure 4. Selective fusion-targeted therapy decreased the tumor size and restored radioiodine uptake in ^{131}I-refractory progressive metastatic pediatric PTCs. Radioactive iodine (RAI) WBS and single-photon emission computed tomography (SPECT) CT scans of a 4.3-year-old girl with *TPR-NTRK1* fusion–positive PTC (**A** and **B**) and a 7.4-year-old girl with *CCDC6-RET* fusion–positive PTC (**C** and **D**). (**A**) The post-treatment WBS showed remnant thyroid uptake only. Radioiodine uptake was restored in the cervical LN and lung lesions after 12 weeks of larotrectinib therapy. (**B**) A CT scan revealed a dramatic improvement in the LN and lung target lesions (decreased to 35% of baseline) after 4 weeks. The patient achieved complete remission after 21 months and remained responsive, with no dose-limiting toxicity seen during 41 months of larotrectinib therapy. (**C**) The post-treatment WBS revealed minimal uptake of radioiodine in the lungs. Radioiodine uptake was restored in the entire lung field after 5 months of selpercatinib treatment (Tx). The addition of ^{131}I (60 mCi) 13 months after starting selpercatinib treatment resulted in remarkable radioiodine uptake in the lung field. (**D**) Lung lesions were markedly improved according to a chest radiograph done 10 days later and decreased to 42.9% of baseline on a CT scan after 4 weeks. The patient achieved partial remission after 4 weeks and remained responsive, with no dose-limiting toxicity seen during 29 months of selpercatinib therapy.

Children with oncogenic fusion PTCs presented with more advanced-stage disease; 42% of the children had lung metastasis and a higher risk for recurrence or persistence than did those with *BRAF*^{V600E} PTC. In particular, among 13 patients with persistent lung metastasis, the disease was stable in 10 patients, while it progressed in 3, despite ^{131}I therapy. Consistent with previous reports (4, 21), the lower TDSs and higher ERK scores demonstrate the aggressiveness of oncogenic fusion PTCs in young children.

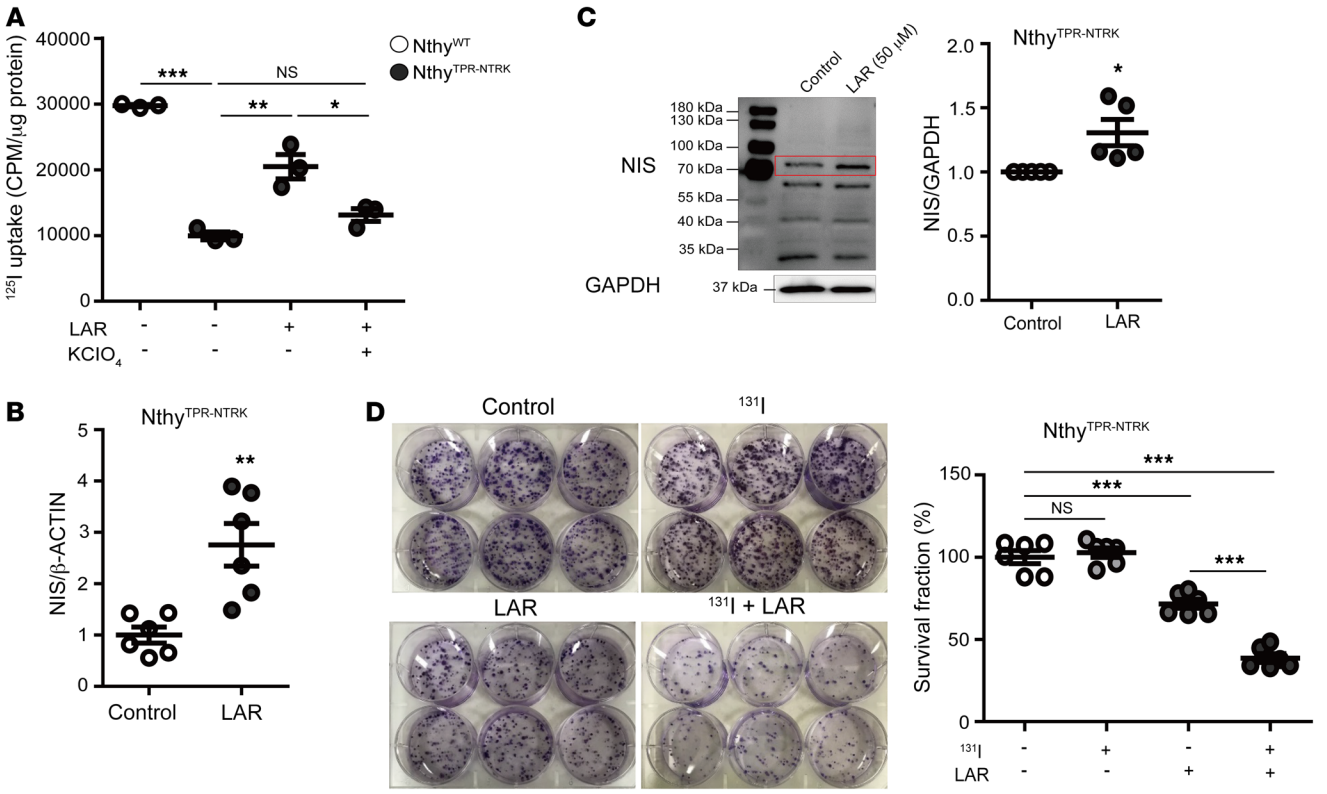

Figure 5. In vitro effects of larotrectinib on radioiodine uptake capacity and cell growth. (**A**) Baseline ^{125}I uptake decreased in Nthy$^{TPR\text{-}NTRK}$ cells compared with Nthy^{WT} cells but was restored by larotrectinib treatment mediated by the NIS; this was demonstrated by blocking the effects with $KClO_4$. Expression of the NIS at the mRNA (**B**) and protein (**C**) levels tended to increase in Nthy$^{TPR\text{-}NTRK}$ cells with larotrectinib (50 μM) treatment. (**D**) The colony-forming ability of Nthy$^{TPR\text{-}NTRK}$ cells did not change after ^{131}I therapy alone but decreased after larotrectinib treatment, and then further decreased after combined ^{131}I and larotrectinib therapy. $^*P < 0.05$, $^{**}P < 0.01$, and $^{***}P < 0.001$, by Student's *t* test or 1-way ANOVA with Bonferroni's multiple-comparison test. All data represent the mean ± standard deviation. LAR, larotrectinib (50 μM).

Although the influence of the *BRAF*^{V600E} mutation alone on tumor aggressiveness remains controversial (21), synergistic effects of *TERT*$^{C228T/C250T}$ and *BRAF*^{V600E} mutations have been shown to lead to a worse prognosis in patients with PTC (26). Therefore, the very low frequency of *TERT*$^{C228T/C250T}$ mutations in pediatric PTCs (2, 3, 5, 7, 17, 20) may explain the less aggressive behavior of pediatric *BRAF*^{V600E} PTCs (21). The reason for the more aggressive nature of pediatric oncogenic fusion PTCs remains unclear.

The low expression of *SLC5A5* (NIS) could explain the radioiodine refractoriness of these tumors. A similar downregulation of thyroid differentiation genes, including *SLC5A5*, has been reported in cases of post-Chernobyl oncogenic fusion PTC (8), although the reported effects of oncogenic fusions on thyroid cancer dedifferentiation are inconsistent (27). It is important to elucidate the genetic alterations and corresponding targeted drugs that most affect the response to ^{131}I therapy depending on NIS expression. In this study, 2 young girls with ^{131}I-refractory progressive PTC and markedly decreased NIS expression exhibited dramatic responses to oncogenic fusion–targeted therapy, which not only decreased tumor size but also restored radioiodine uptake.

The tumor responses in this study were consistent with previous reports of patients with TRK fusion–positive thyroid cancer treated with larotrectinib (9, 28) and a recent report on patients with *RET*-altered medullary thyroid cancer treated with selpercatinib (29). Surprisingly, however, the combination of selpercatinib and ^{131}I therapy enhanced radioiodine uptake and yielded a remarkable tumor response in a girl with PTC harboring a *CCDC6-RET* fusion, implying that selpercatinib could be an effective redifferentiation therapy in ^{131}I-refractory advanced tumors harboring the *RET* fusion oncogene. The treatment response decreased after the third ^{131}I treatment in a 9-year-old boy (P11) recruited for a clinical trial of fusion-targeted therapy. Assuming restoration of ^{131}I avidity in the girl harboring the *RET* fusion oncogene, it would have been helpful if the 9-year-old boy had received selpercatinib in combination with the third ^{131}I treatment. In vitro experiments also support the efficacy of larotrectinib for restoring NIS expression and radioiodine avidity, in addition to inhibiting tumor growth. Therefore, this study supports further investigation of fusion-targeted therapy for redifferentiation of ^{131}I-refractory progressive thyroid cancer (14–16). Our pediatric cases are in agreement with a recent adult case report on larotrectinib-enhanced ^{131}I uptake in advanced PTC (30). Considering the predominance of oncogenic fusions in pediatric patients with PTC and their association with tumor aggressiveness, recently developed, potent, and specific kinase inhibitors targeting oncogenic fusions in PTC could be the optimal therapeutic option for ^{131}I-refractory advanced PTCs in children. Furthermore, reactivation of radioiodine uptake indicates that ^{131}I therapy combined with fusion-targeted therapy can

be effective in previously ^{131}I-refractory PTC patients (30). Targeted oncogene therapies before surgery may induce tumor regression in cases of invasive thyroid cancer (31). Diagnostic molecular testing to detect driver oncogenic fusions and point mutations is becoming imperative in such cases.

This study was limited by the small number of fresh pediatric tissue samples, so the difference in gene expression between pediatric and adult PTCs needs to be further replicated in a large-sample study. To date, there are no available published data on pediatric PTCs allowing comparison of gene expression with that in adult PTCs. In addition, various methods were applied to identify the genetic alterations, due to issues with tissue availability and sample quality, particularly in the NGS-failed FFPE tissue samples. Although the use of FISH, IHC, and direct sequencing is beneficial for detecting *RET* or *ALK* fusions and the *DICER1* variant (Supplemental Table 1), there may have been unidentified genetic drivers in the NGS-failed samples (n = 15), leading to an underestimation of the detection rate in our study. Nonetheless, to our knowledge, this is the first pediatric study to show that fusion-targeted therapy reactivated radioiodine uptake and inhibited tumor growth in patients with ^{131}I-refractory PTC. In addition, we performed an in vitro experiment to demonstrate the role of fusion-targeted therapy in restoring NIS expression and radioiodine uptake.

In summary, oncogenic fusions are the main genetic drivers of PTCs identified in young children. Selective fusion-targeted therapy may restore radioiodine avidity, as well as produce a tumor response in pediatric fusion oncogene PTCs with ^{131}I-refractory advanced characteristics, making molecular testing imperative for pediatric patients presenting with advanced PTC.

Methods

Patients and tissue samples. In total, we analyzed 106 tumor tissue samples from pediatric patients with PTC, obtained at the SNUH between January 1983 and March 2020 (Figure 1). Fresh-frozen tumor tissue samples were obtained from 12 pediatric patients under the age of 20 years. The transcriptomic data on adult patients aged 20 years or older (125 cases at SNUH) were analyzed to compare gene expression profiles (11). Detailed information on the treatment and follow-up strategies was obtained (12), and disease outcomes were categorized as no evidence of disease (NED), BCD, or persistent or recurrent SD (32), as described in the Supplemental Methods.

Genomic profiling by NGS, direct sequencing, FISH, and/or IHC. Genetic analysis was performed using whole-genome sequencing (WGS), targeted sequencing, RNA-Seq, direct sequencing, FISH, and/or IHC according to the tissue availability (Figure 1 and Supplemental Table 1). RNA-Seq libraries of fresh-frozen and FFPE tissues were constructed using the TruSeq RNA Library Preparation Kit, version 2, and the TruSeq RNA Access Library Preparation Kit (both from Illumina), respectively. The TruSeq Nano DNA Preparation Kit (Illumina) was used to construct the library for WGS. The subsequent NGS analysis is described in the Supplemental Methods. The *BRAF* exon 15, *TERT* promoter (C228T and C250T) region, *H/K/NRAS* codons 12, 13, and 61, and the sequence encoding the *DICER1* RNase IIIb domain were amplified by PCR using the appropriate primers for direct sequencing of the *BRAF*, *RAS*, *DICER1*, and *TERT* genes (Supplemental Table 8) (18). Supplemental Table 9 lists the target genes for the SNUH FIRST cancer panel (version 3). The FISH probe for the *NTRK* and *RET* rearrangements and the antibodies for IHC of *BRAF*^{V600E}, *NRAS* Q61R, *ALK*, and *pan-Trk* are described in the Supplemental Methods.

Cell culturing and in vitro assays. The human *TPR-NTRK1* expression vector was constructed by subcloning the corresponding cDNAs into the pcDNA6/V5-His A expression vector (Thermo Fisher Scientific) (Supplemental Figure 5 and Supplemental Table 5). The pcDNA6/V5-His A-TPR-NTRK1 fusion construct Nthy$^{TPR\text{-}NTRK}$ and the unmodified vector control pcDNA6/V5-His A (Nthy^{WT}) were transfected into N-thyroid cells (European Collection of Authenticated Cell Cultures [ECACC]). The degree of overexpression of Nthy$^{TPR\text{-}NTRK}$ cells was similar to that seen in NTRK fusion cancer, based on comparison of the *NTRK* mRNA levels in Nthy^{WT} cells, normal thyroid tissue, Nthy$^{TPR\text{-}NTRK}$ cells, and thyroid cancer tissues with a TPR-NTRK fusion (Supplemental Figure 6).

After incubation with larotrectinib (provided by Bayer AG), mRNA and protein expression levels and ^{125}I uptake were analyzed. ^{131}I clonogenic assays were performed in Nthy$^{TPR\text{-}NTRK}$ or Nthy^{WT} transfected cells, as described previously (33). NIS mRNA and protein expression was analyzed by reverse transcriptase PCR (RT-PCR) (using the appropriate primers; see Supplemental Table 8) and immunoblotting with an anti-NIS antibody (Thermo Fisher Scientific), respectively.

Statistics. All analyses were performed using SPSS software for Windows (version 25.0). Differences in continuous variables were compared between 2 groups using a 2-tailed Student's t test or a Mann–Whitney U test. Categorical variables were compared between the 2 groups using the χ^2 or Fisher's exact test, whereas the χ^2 test for trend or logistic regression was used for comparisons among 3 groups. Recurrence-free survival plots were constructed using the Kaplan-Meier method, and groups were compared using the Cox proportional hazards model. The HRs, 95% CIs, and P values are reported in the figures and legends. A P value of less than 0.05 was considered significant.

Data availability. The RNA-Seq data set produced in this study was deposited in the NCBI's Sequence Read Archive (SRA PRJNA701374).

Study approval. Written informed consent for participation in this study was obtained from patients or their parents or guardians, as required by the SNUH IRB (approval IDs: H-1307-034-501, 1505-023-670).

Author contributions

YAL, JIK, and YJP conceived and designed the study. HL, SWI, and JC analyzed NGS data under the supervision of JIK. YAL, DYO, HJK, JKW, KCJ, DK, EJC, JHH, JCP, JHK, CHS, and YJP delivered multidisciplinary therapy to pediatric patients with thyroid cancer, prepared tissue samples, explored the pathologies in play, and collected imaging data. In particular, DYO and HJK delivered fusion-directed targeted therapy. OHK, JMO, and BCA performed the in vitro experiment. YAL, HL, SWI, YSS, JIK, and YJP drafted the manuscript. LJW contributed to data interpretation and manuscript revision. All authors contributed to multiple revisions of the manuscript and approved the final version. The corresponding authors, JIK and YJP, had full access to all the data in the study and had final responsibility for the decision to submit it for publication.

Acknowledgments

All research, except the clinical trials for the 2 patients with progressive ^{131}I-refractory lung metastases harboring a *TPR-NTRK1* or *CCDC6-RET* fusion who received fusion-targeted therapy

with larotrectinib (NCT02576431; NAVIGATE) or selpercatinib (LOXO-RET-18018), was supported by the Basic Science Research Program through the National Research Foundation of Korea (NRF), funded by the Ministry of Science, ICT and Future Planning (NRF-2016R1A2B4012417 and 2019R1A2C2084332); a grant from the Korea Health Technology R&D Project through the Korea Health Industry Development Institute (KHIDI), funded by the Ministry of Health and Welfare, Republic of Korea (H14C1277); and the Basic Science Research Program through the NRF, funded by the Ministry of Education (2020R1A6A1A03047972). This study was also supported by the SNUH Research Fund (grant no. 04-2015-0830). The authors thank Bayer AG and Eli Lilly and Company for medical monitoring of the patients treated with larotrectinib and selpercatinib, respectively. The authors especially thank Jeong Seon Lee, Hwan Hee Kim, Gyeongseo Jung, and Sookyung Kim for sample preparation and molecular analyses.

Address correspondence to: Young Joo Park, Department of Internal Medicine, Seoul National University College of Medicine, 101 Daehak-ro, Jongno-gu, Seoul 03080, Republic of Korea. Phone: 82.2.2072.4183; Email: yjparkmd@snu.ac.kr. Or to: Jong-Il Kim, Department of Biomedical Sciences, Seoul National University Graduate School, 103 Daehak-ro, Jongno-gu, Seoul 03080, Republic of Korea. Phone: 82.740.8421; Email: jongil@snu.ac.kr.

1. Bauer AJ. Molecular genetics of thyroid cancer in children and adolescents. *Endocrinol Metab Clin North Am*. 2017;46(2):389–403.
2. Paulson VA, et al. Thyroid cancer in the pediatric population. *Genes (Basel)*. 2019;10(9):E723.
3. Pozdeyev N, et al. Genetic analysis of 779 advanced differentiated and anaplastic thyroid cancers. *Clin Cancer Res*. 2018;24(13):3059–3068.
4. Prasad ML, et al. NTRK fusion oncogenes in pediatric papillary thyroid carcinoma in northeast United States. *Cancer*. 2016;122(7):1097–1107.
5. Picarsic JL, et al. Molecular characterization of sporadic pediatric thyroid carcinoma with the DNA/RNA ThyroSeq v2 next-generation sequencing assay. *Pediatr Dev Pathol*. 2016;19(2):115–122.
6. Ballester LY, et al. Integrating molecular testing in the diagnosis and management of children with thyroid lesions. *Pediatr Dev Pathol*. 2016;19(2):94–100.
7. Pekova B, et al. Somatic genetic alterations in a large cohort of pediatric thyroid nodules. *Endocr Connect*. 2019;8(6):796–805.
8. Ricarte-Filho JC, et al. Identification of kinase fusion oncogenes in post-Chernobyl radiation-induced thyroid cancers. *J Clin Invest*. 2013;123(11):4935–4944.
9. Drilon A, et al. Efficacy of larotrectinib in TRK fusion-positive cancers in adults and children. *N Engl J Med*. 2018;378(8):731–739.
10. Drilon A, et al. Targeting RET-driven cancers: lessons from evolving preclinical and clinical landscapes. *Nat Rev Clin Oncol*. 2018;15(3):150.
11. Yoo SK, et al. Comprehensive analysis of the transcriptional and mutational landscape of follicular and papillary thyroid cancers. *PLoS Genet*. 2016;12(8):e1006239.
12. Lee YA, et al. Pediatric patients with multifocal papillary thyroid cancer have higher recurrence rates than adult patients: a retrospective analysis of a large pediatric thyroid cancer cohort over 33 years. *J Clin Endocrinol Metab*. 2015;100(4):1619–1629.
13. Cancer Genome Atlas Research Network. Integrated genomic characterization of papillary thyroid carcinoma. *Cell*. 2014;159(3):676–90.
14. Ho AL, et al. Selumetinib-enhanced radioiodine uptake in advanced thyroid cancer. *N Engl J Med*. 2013;368(7):623–632.
15. Rothenberg SM, et al. Redifferentiation of iodine-refractory BRAF V600E-mutant metastatic papillary thyroid cancer with dabrafenib. *Clin Cancer Res*. 2015;21(5):1028–1035.
16. Dunn LA, et al. Vemurafenib redifferentiation of BRAF mutant, RAI-refractory thyroid cancers. *J Clin Endocrinol Metab*. 2019;104(5):1417–1428.
17. Pekova B, et al. RET, NTRK, ALK, BRAF and MET fusions in a large cohort of pediatric papillary thyroid carcinomas. *Thyroid*. 2020;30(12):1771–1780.
18. Song YS, et al. Prognostic effects of TERT promoter mutations are enhanced by coexistence with BRAF or RAS mutations and strengthen the risk prediction by the ATA or TNM staging system in differentiated thyroid cancer patients. *Cancer*. 2016;122(9):1370–1379.
19. Wasserman JD, et al. DICER1 mutations are frequent in adolescent-onset papillary thyroid carcinoma. *J Clin Endocrinol Metab*. 2018;103(5):2009–2015.
20. Alzahrani AS, et al. Uncommon TERT promoter mutations in pediatric thyroid cancer. *Thyroid*. 2016;26(2):235–241.
21. Alzahrani AS, et al. Single point mutations in pediatric differentiated thyroid cancer. *Thyroid*. 2017;27(2):189–196.
22. Cordioli MI, et al. Fusion oncogenes are the main genetic events found in sporadic papillary thyroid carcinomas from children. *Thyroid*. 2017;27(2):182–188.
23. Nikiforov YE, Nikiforova MN. Molecular genetics and diagnosis of thyroid cancer. *Nat Rev Endocrinol*. 2011;7(10):569–580.
24. Roukos V, Misteli T. The biogenesis of chromosome translocations. *Nat Cell Biol*. 2014;16(4):293–300.
25. Efanov AA, et al. Investigation of the relationship between radiation dose and gene mutations and fusions in post-Chernobyl thyroid cancer. *J Natl Cancer Inst*. 2018;110(4):371–378.
26. Xing M, et al. BRAF V600E and TERT promoter mutations cooperatively identify the most aggressive papillary thyroid cancer with highest recurrence. *J Clin Oncol*. 2014;32(25):2718–2726.
27. Romei C, et al. BRAFV600E mutation, but not RET/PTC rearrangements, is correlated with a lower expression of both thyroperoxidase and sodium iodide symporter genes in papillary thyroid cancer. *Endocr Relat Cancer*. 2008;15(2):511–520.
28. Hong DS, et al. Larotrectinib in patients with TRK fusion-positive solid tumours: a pooled analysis of three phase 1/2 clinical trials. *Lancet Oncol*. 2020;21(4):531–540.
29. Wirth LJ, et al. Efficacy of selpercatinib in *RET*-altered thyroid cancers. *N Engl J Med*. 2020;383(9):825–835.
30. Groussin L, et al. Larotrectinib-enhanced radioactive iodine uptake in advanced thyroid cancer. *N Engl J Med*. 2020;383(17):1686–1687.
31. Kazahaya K, et al. Targeted oncogene therapy before surgery in pediatric patients with advanced invasive thyroid cancer at initial presentation: is it time for a paradigm shift? *JAMA Otolaryngol Head Neck Surg*. 2020;146(8):748–753.
32. Jeon MJ, et al. Practical initial risk stratification based on lymph node metastases in pediatric and adolescent differentiated thyroid cancer. *Thyroid*. 2018;28(2):193–200.
33. Oh JM, et al. Reverting iodine avidity of radioactive-iodine refractory thyroid cancer with a new tyrosine kinase inhibitor (K905-0266) excavated by high-throughput NIS (sodium iodide symporter) enhancer screening platform using dual reporter gene system. *Oncotarget*. 2018;9(6):7075–7087.